Measurement and Prediction of Model-Rotor Flowfields

F. Kevin Owen* and Michael E. Tauber†
NASA Ames Research Center, Moffett Field, California

A laser velocimeter was used to measure accurately the three-component velocities induced by a model rotor at transonic tip speeds. The measurements, which were made at Mach numbers 0.85–0.95 and at zero advance ratio, yielded high-resolution, orthogonal velocity values. The measured velocities were used to check the ability of the ROT22 full-potential rotor code to predict the transonic flowfield in the crucial region around and beyond the tip of a high-speed rotor blade. The good agreement between the calculated and measured velocities established the code's ability to predict the off-blade flowfield at transonic tip speeds. This supplements previous comparisons in which surface pressures were shown to be well predicted on two different tips at advance ratios of 0.40 and 0.45, especially at the critical 90-deg azimuthal blade position. These results demonstrate that the ROT22 code can be used to predict the important tip-region flowfield, including the occurrence, strength, and location of shock waves causing high drag and noise.

Introduction

THE emphasis on increasing helicopter flight speed has resulted in extensive regions of transonic flow in the vicinity of the tips of the advancing rotor blade. However, it is essential that these desired performance improvements be achieved with reasonable power requirements and without substantial increases in noise. Since the formation of shock waves in the transonic flow on the advancing blade is at once the major cause of the power requirements and the principal source of high-speed noise, an ability to predict the flowfield well is essential to the design of efficient transonic rotors.

The objective of the present study was to measure the transonic flowfield near the blade tip, using nonintrusive laser velocimetry, and to compare the data with computations from the ROT22 transonic rotor flow code.[1,2] Since a precise definition of the velocity field surrounding the blade tip is required to calculate transonic noise, nonintrusive laser velocimeter measurements provide the only reasonable means of checking the ROT22 code's ability to predict the velocities off the blade surface. The measurements were made on a nonlifting, hovering rotor at tip Mach numbers from 0.85 to 0.95.[3] Previously, comparisons of measured and calculated surface-pressure distributions on straight and swept-back rotor tips at advance ratios of 0.4 and 0.45 (corresponding to very high-speed forward flight) showed good agreement.[4]

A description of the experimental procedure used to determine the velocities in the flowfield is presented, followed by a brief discussion of the development, features, and simplifying assumptions of the ROT22 codes. Comparisons of measured and calculated velocity fields at two positions above the blade and at three blade radial stations are presented and discussed.

Description of Experiment

Test Conditions and Model Configuration

The test was performed in the Ames/Army Aeromechanics Laboratory hover facility, which is a large chamber, about 10 m square, with special ducting designed to minimize room circulation. The two-bladed rotor, which was located in the center of the room, was mounted on a tall column containing the drive shaft. The rotor consisted of two cantilever-mounted, manually adjustable blades. The blades, which were untwisted and untapered, had NACA 0012 airfoil sections and an aspect ratio of 12. The rotor radius and chord were 104.5 cm (41.16 in.) and 7.62 cm (3.0 in.), respectively.

The induced velocities were measured at tip Mach numbers of 0.85, 0.88, 0.90, and 0.95. The blade was set at a positive collective pitch angle of 1.25 deg to convect the viscous wake slightly downward and reduce the turbulence in the plane of rotation. However, the effective angle of incidence in the tip region of the blade was estimated to be less than 0.5 deg. The measurements were made in a volume 1 chord (7.62 cm) high and extending from the 95% blade radius location (5.23 cm inboard of the tip) to the sonic circle. Although most of the velocity measurements were made above the blade, a limited number were also made below the blade to determine the extent of flow asymmetry. In hover the location of the unperturbed sonic circle[5] is given by

$$S = 1/M_{TIP} \tag{1}$$

where S is measured in blade radii from the center of rotation and M_{TIP} is the rotational tip Mach number. The distance of the sonic circle from the blade tip varied from 7.26 cm at a tip Mach number of 0.85 to 2.17 cm at a Mach number of 0.95. Since the location of the sonic circle is critically important in the transmission of impulsive noise into the far field, it is essential to check the code's ability to calculate the flow in this region accurately.

Measurement Technique

The general arrangement of the laser velocimeter system used in the present study is shown in Fig. 1. This fringe-mode, forward-scatter system, which utilized the 4880- and 5145-Å lines of an argon-ion laser, was specifically designed to measure all three components of induced perturbation velocity by measuring the flow at two different azimuthal positions. By viewing normal to the tip as it swept by, one spectral line measured the induced chordwise velocity component and the other measured the induced vertical velocity component. Translation of both transmitting and receiving optics along the test chamber walls enabled a flowfield view normal to the approaching or retreating tip, thus determining the radial and vertical induced velocities. The effective sensing volume was approximately elliptic, 0.2 mm in diameter and 3 mm long, with the axis aligned in the plane of the beams. Bragg-cell frequency shifting, which is required for probing directionally intermittent flowfields, was incorporated in both spectral lines.

Presented as Paper 85-1558 at the AIAA 18th Fluid Dynamics, Plasmadynamics and Lasers Conference, Cincinnati, OH, July 16–18, 1985; received Jan. 7, 1986; revision received July 30, 1986.

*Presently, President, Complere Inc., Palo Alto, CA. Member AIAA.

Maximum optical system sensitivity is essential for valid measurements, particularly in large facilities. In such facilities, solid-angle light collection is reduced, raising the possibility that only the velocities of larger particles, which may not follow the flow, will be observed. Rather than relying entirely on natural aerosols for the light scattering, it was found that the introduction of artificial aerosols of known size distribution greatly enhanced data-acquisition rates, particularly in unsteady flows where conditional sampling had to be used. The aerosols were generated by passing high-frequency waves through nozzles submerged in the seeding liquid. The size distribution of the resulting aerosol is shown in Fig. 2; the peak aerodynamic mean diameter is less than 1 μm. Aerosols of these dimensions had been found adequate for turbulence studies of shock/boundary-layer interactions and of vortex flows at transonic and supersonic speeds.[6] The particles were drawn down through the laser velocimeter focal volume by the room air-control fans. This produced a sufficient supply of scattering centers for detailed flowfield measurements.

Data Acquisition and Reduction

The data-acquisition and reduction system consisted primarily of three elements: signal processors, an event synchronizer, and a desktop computer. These elements are shown schematically in Fig. 3. Conditional sampling techniques were employed to "freeze" the flowfield as the rotor swept past the fixed probe volume. To achieve this, a once-per-revolution pulse was used to activate the laser velocimeter electronics each time the rotor approached the probe focal volume. Velocities were then recorded while the rotor moved past the focal volume. After the preset time had elapsed, the electronics were inhibited until the next rotor passage.

A schematic of the two-component measurement procedure used in the present test is shown in Fig. 4. The internal clock of the event synchronizer (multiplexer), which was reset by an external pulse from the rotor drive mechanism, determined the position of the blade relative to the measurement volume. Whenever valid (essentially simultaneous) u and v signals were received, the velocity data along with the clock reading (which corresponded to the chordwise position of the measurement volumes) were recorded. From these readings, ensemble averages were generated for the selected chordwise increments along the blade. It must be borne in mind that the measurements were made by collecting data over many blade revolutions, since the data rate was insufficient and too inconsistent to obtain enough information at each chordwise location for each blade passage. For this reason, the total number of readings per blade passage was divided among many incremental blade positions. Typically, some of these chordwise "windows" would fill more quickly than others. However, new readings were accepted, and they replaced the oldest data until all chordwise locations were filled. This ensured that only the most current data were retained. The data contained the information required to determine the instantaneous velocities. From these determinations, the average velocities, rms turbulence levels, and cross-correlations could all be calculated.

The orthogonal induced velocity components were measured in an inertial (room-fixed) coordinate system. However, aerodynamic properties of moving bodies are normally calculated in body-fixed coordinates. Therefore, the measured velocity components were transformed into blade-fixed coordinates by using the following expressions:

$$u = v_m + \omega r$$

$$v = v_m$$

$$w = w_m - \omega x \tag{2}$$

Here, u, v, and w are the chordwise, vertical, and radial velocity components, respectively. The subscript m refers to measured values, ω is the blade-rotation rate, r the blade radius from the center of rotation, and x the chordwise distance from the leading edge.

At each location relative to the leading edge of the blade and the centerline of the airfoil, a horizontal velocity component (either u or w) and the vertical one, v, were measured. Between 2000 and 8000 instantaneous measurements were averaged to determine each data point within the velocity distribution; thus, test time limitations precluded measuring all three velocity components at each location. Because the LV system had to be moved and realigned when changing horizontal velocity component (u or w) measurements, only u and v, or w and y values were determined at many locations. The greatest difficulty was encountered in measuring v, because light reflecting off the blade surface severely degraded the signal when scanning near the blade.

When measurements were made in the vicinity of the shock, the velocity probability density functions exhibited revolution-to-revolution flowfield variations. This unsteadiness of the flowfield was noted because data were collected over a large number of rotations. The flowfield variability may have been caused by the presence of a transitional boundary layer, since

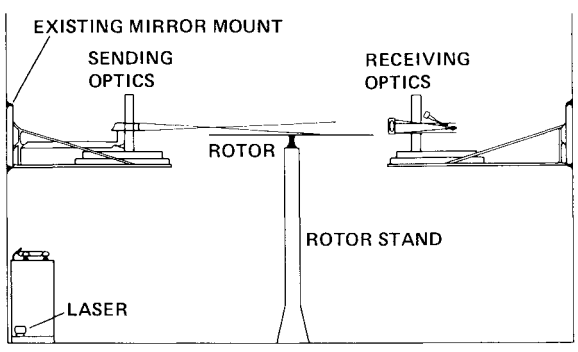

Fig. 1 Model rotor test setup showing laser velocimeter system.

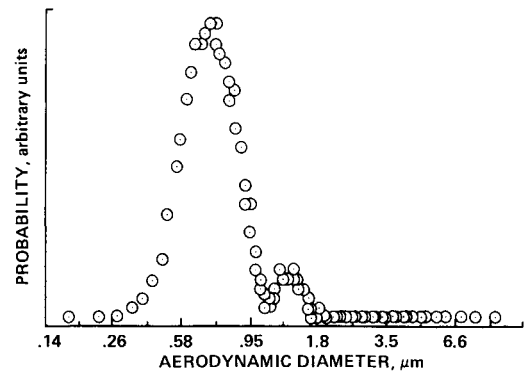

Fig. 2 Seed particle size distribution.

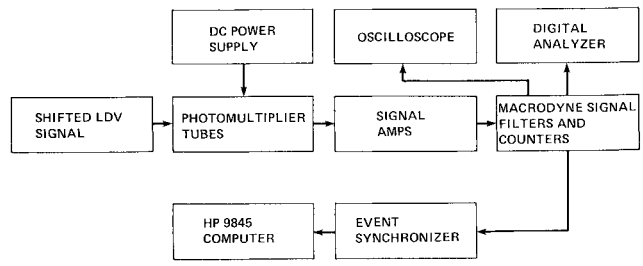

Fig. 3 Data-acquisition system.

the chord Reynolds numbers in the blade-tip region were only 1.5×10^6 to 1.75×10^6 and no artificial trips were used. In fact, holographic measurements made under very similar test conditions[7] indicated the presence of lambda shocks and subsequent flow separation. Flow unsteadiness is often associated with shock-induced boundary-layer separation,[6] and it could be inferred from some of the histograms obtained during the present test. An estimate of the inherent revolution-to-revolution flowfield repeatability could be made by comparing the measured and the most likely velocity probability density functions. Such comparisons are reported in Ref. 3, which showed that in blade coordinates, the maximum differences in the measured chordwise velocities u were less than 10%. The effects on the vertical velocity v and the radial velocity w were negligible.

Therefore, the measurements were analyzed in terms of the most likely probability density function profiles, which were somewhat sharper with lower rms levels. Because this approach tended to suppress some of the viscous effects, the comparison provided a more realistic test of the inviscid calculational procedure.

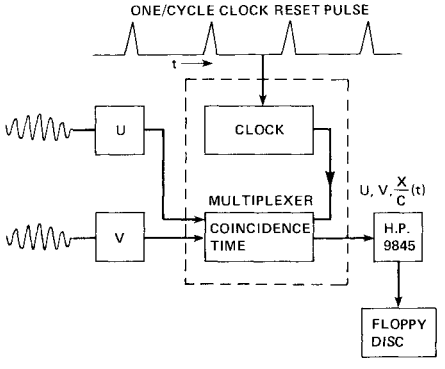

Fig. 4 Conditional sampling system.

Computations

Early high-speed rotor calculations were performed by Caradonna and Isom[8,9] using transonic small-disturbance theory. Initially, steady hovering flight was treated[8]; this was later extended to the unsteady forward flight case.[9] Subsequently, Grant[10] solved the small-disturbance equation more precisely but assumed quasisteady flow for a blade in nonlifting forward flight.

Paralleling the development of fixed-wing flowfield codes, for the rotary-wing case, it was also desirable to progress from using small-disturbance theory to solving the full-potential equation. As a starting point, a widely used full-potential, fixed-wing code, FLO22, developed by Jameson and Caughey,[11] was used. FLO22 solves the nonconservative, inviscid, full-potential equation using exact surface tangency boundary conditions. (In a comparison of inviscid, full-potential, fixed-wing codes, it was shown[12] that nonconservative formulations predicted shock strengths and locations better than conservative, finite-volume, methods.) The rotary-wing code ROT22 was developed by reformulating FLO22 to calculate the flow about a lifting rotor blade in forward flight. (The utility of ROT22 has recently been enhanced by coupling the code with an improved and extended far wake, as described in Ref. 13.) Although the full-potential equation is solved, the formulation is quasisteady in that the time derivatives of the perturbation potentials were neglected in the interest of greatly speeding up the computation. However, the ROT22 quasisteady approximation becomes exact for hovering flight corresponding to the zero-advance-ratio condition of the experiment.

Using the ROT22 code, the flowfield over the entire blade was calculated for the tip Mach numbers of the experiment. A computational grid of 120 cells chordwise, 16 vertically, and 32 spanwise was used. About two-thirds of the spanwise computational planes were on the blade; the remainder were in the inboard cutout and beyond the blade tip. Nonlinear spanwise grid spacing was used to enhance the resolution in the tip region and to place a computational plane at the 95% radial blade station where one set of measurements was made. At the

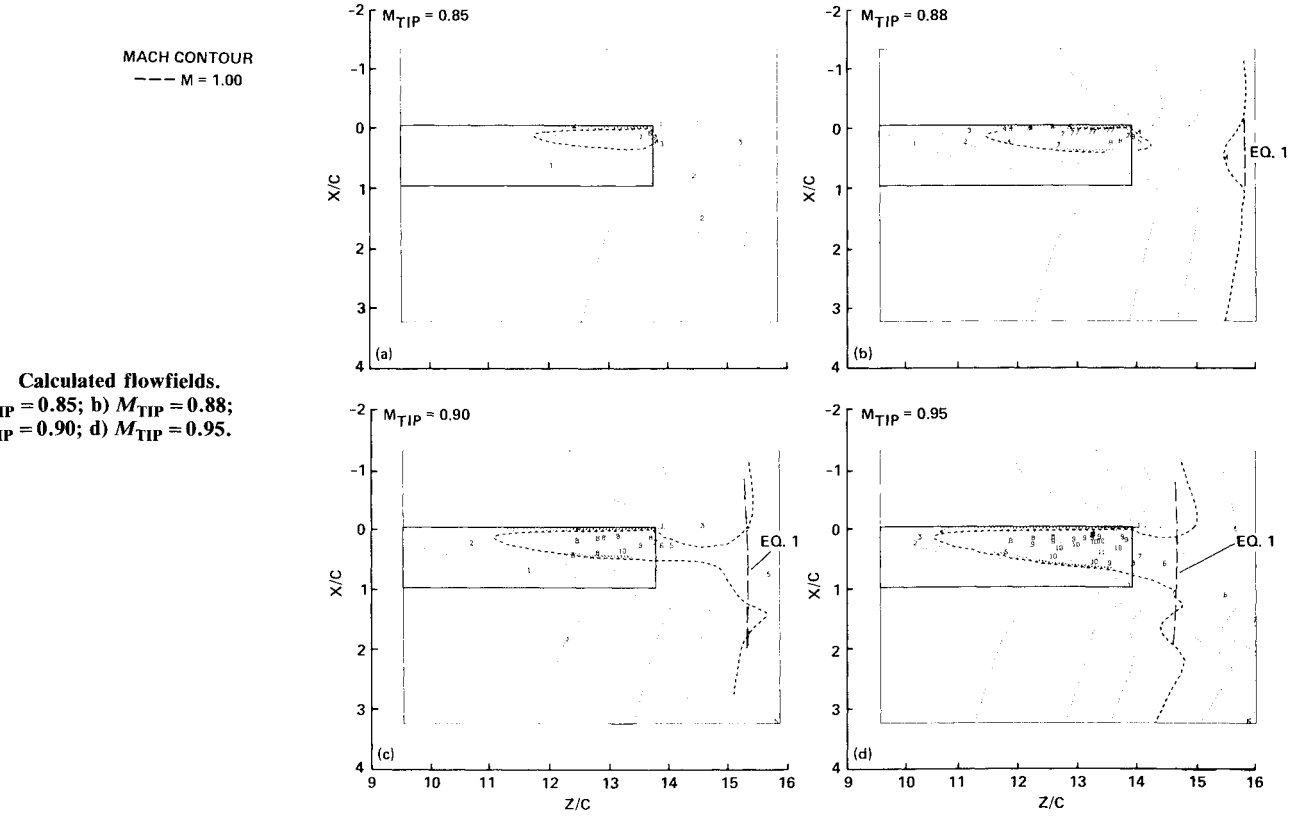

Fig. 5 Calculated flowfields.
a) $M_{TIP}=0.85$; b) $M_{TIP}=0.88$; c) $M_{TIP}=0.90$; d) $M_{TIP}=0.95$.

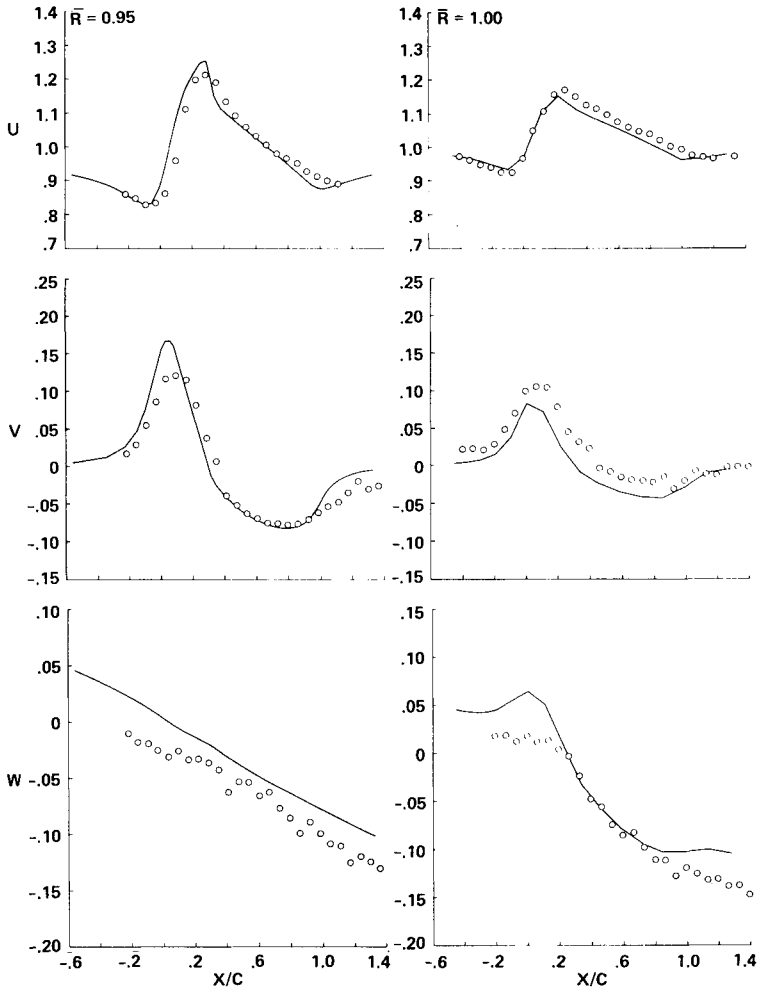

Fig. 6a Comparison of ROT22 calculated velocities with LV measurements: $M_{TIP} = 0.85$, $Y/C = 0.1505$.

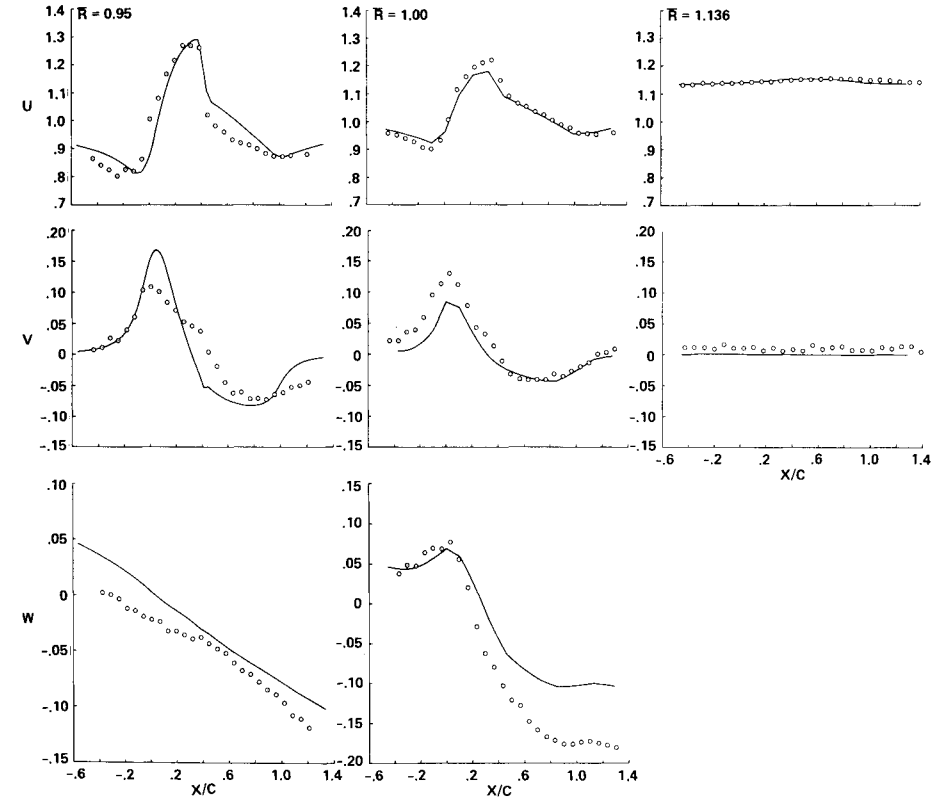

Fig. 6b Comparison of ROT22 calculated velocities with LV measurements: $M_{TIP} = 0.88$, $Y/C = 0.1505$.

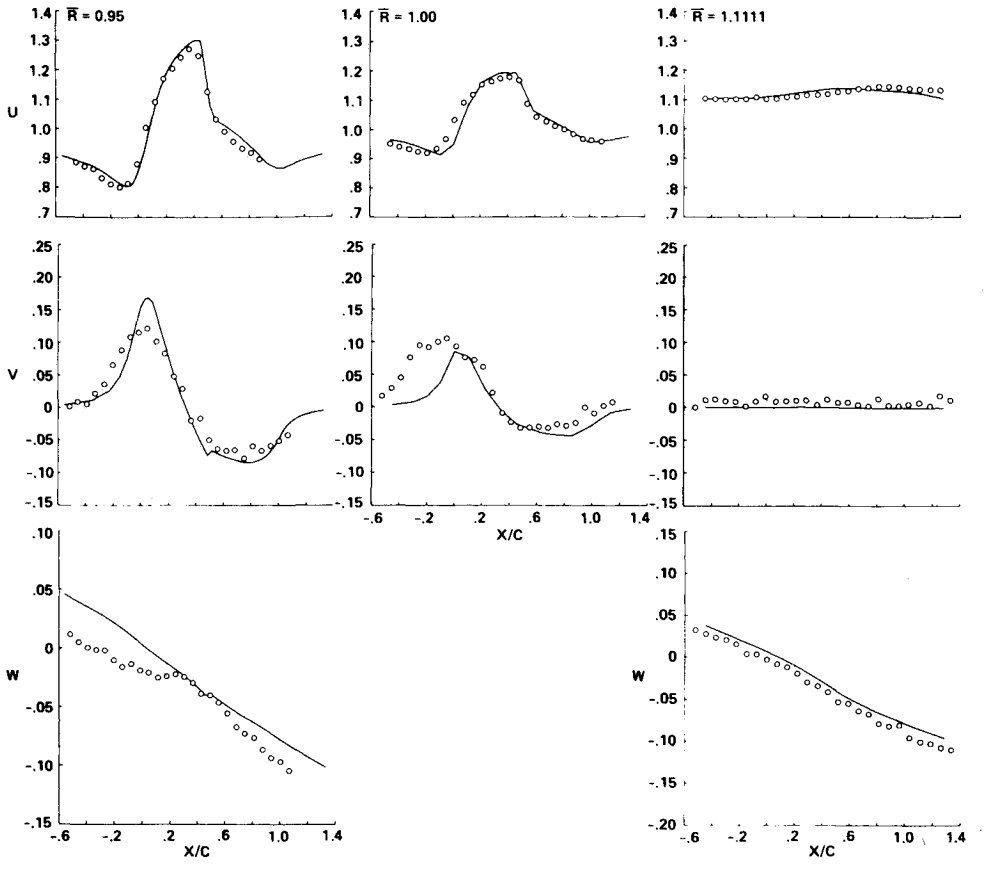

Fig. 6c Comparison of ROT22 calculated velocities with LV measurements: $M_{TIP}=0.90$, $Y/C=0.1505$.

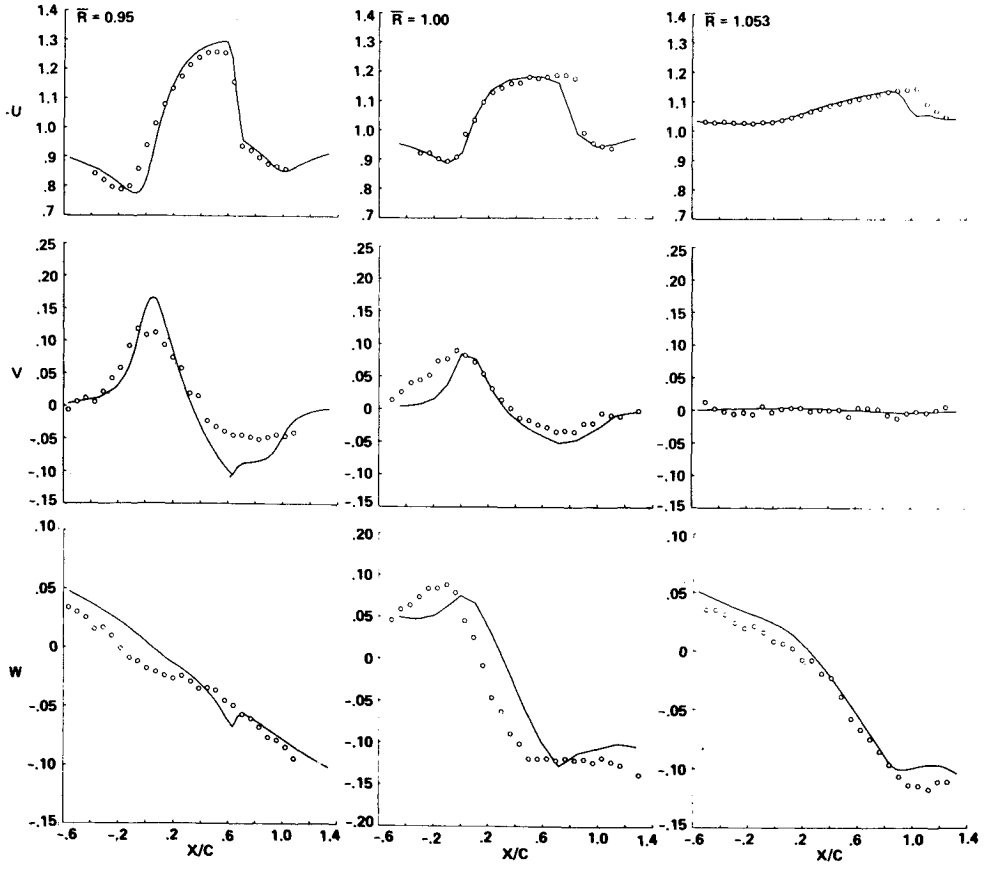

Fig. 6d Comparison of ROT22 calculated velocities with LV measurements: $M_{TIP}=0.95$, $Y/C=0.1505$.

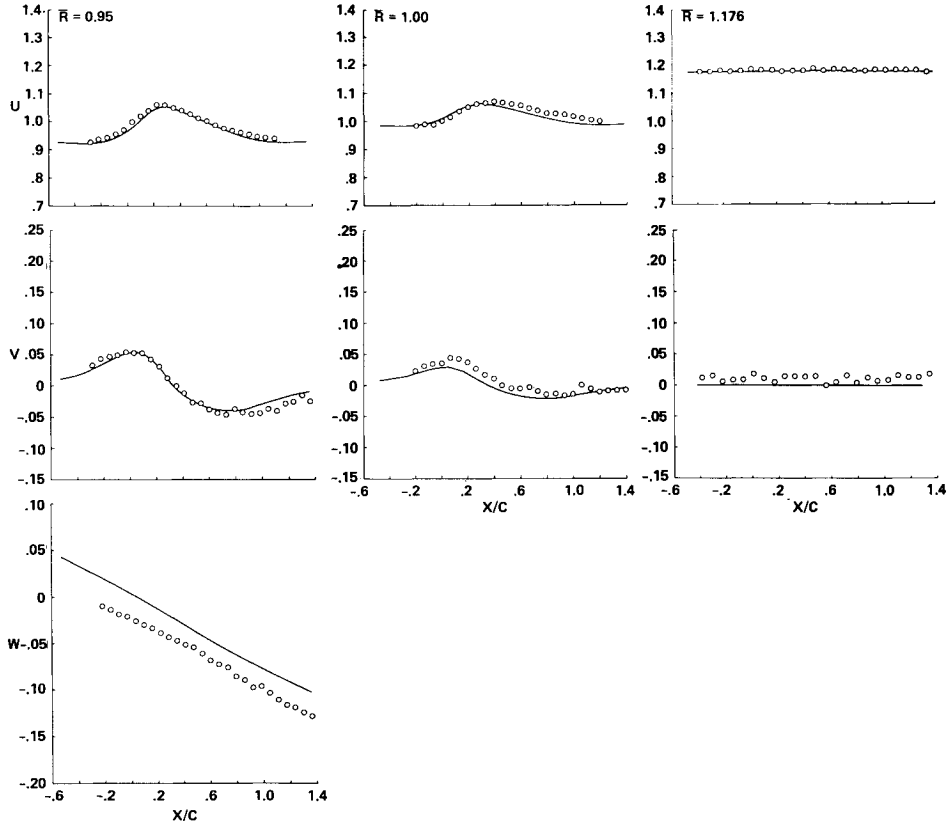

Fig. 6e Comparison of ROT22 calculated velocities with LV measurements: $M_{TIP} = 0.85$, $Y/C = 0.5172$.

remaining radial measurement stations, located at the blade tip and idealized sonic cylinder [Eq. (1)], the velocities were calculated by linearly interpolating between adjacent computational planes. The interpolated velocities were then compared with the experimental values. (It was undesirable to place a computational plane at the blade tip, since the velocity gradients were very steep at that location.) Likewise, linear interpolation was used within the physically nonorthogonal computational grid to match the locations of the vertical measurements stations. All computations were made assuming zero collective pitch; since the airfoil section was symmetric, this resulted in no lift.

The computed results consisted of the u, v, and w velocity components, nondimensionalized by the rotational tip speed, and the pressure coefficient and local Mach number. For the present comparisons, special provisions were made for (linearly) interpolating between computational mesh points for the velocity components along horizontal lines of constant y and between vertical planes. An efficient, fully vectorized version of the code on a Cray XM-P computer required computation times of 30–40 s/case.

Results and Discussion

The flowfield over the entire blade was calculated for the four tip Mach numbers of the experiment: 0.85, 0.88, 0.90, and 0.95. The complexity of the flowfield for even this simple case of a nonlifting blade at zero advance ratio is illustrated in Fig. 5. Here, calculated contours of constant Mach number were plotted on the blade surface and in the plane of the blade for all four tip Mach numbers. The calculations were made for the entire blade but, in the interest of clarity, only the tip regions are shown. Note that for a tip Mach number of 0.90 and higher, the supersonic region on the blade merges with the far-field supersonic flow beyond the tip. (Since the ROT22 calculations were in a blade-attached coordinate system, the flowfield is shown as it would appear to an observer stationed on the blade.) This phenomenon, labeled "delocalization" in Ref. 5, permits shock waves forming on the blade to propagate into the far field, thus producing impulsive noise.[5] Also, the flow perturbations caused by the blade strongly affected the region beyond the tip, causing a significant distortion of the simple, unperturbed, sonic circle predicted by Eq. (1). Although the comparisons were made for a nonlifting blade in hover, the results should also be applicable to the more realistic forward-flight case. Delocalization, which is predominantly a function of tip Mach number,[5] was most likely at the 90-deg blade position in forward flight; at this azimuth, the angle of incidence of the blade tip is normally very small and has little effect on the flow beyond the tip.[14]

To present a clear description of the flowfield in the critical tip region of the blade, the three orthogonal velocity components are compared at all three spanwise stations at a given height above the airfoil's centerline at each tip Mach number. However, since measurements were not made of all three velocities and at all three spanwise stations, comparisons of theory and experiment are shown only when data were available.

The comparisons are presented at each tip Mach number for scans 0.15 chord lengths (Figs. 6a and 6b) and 0.52 chord lengths (Figs. 6e–6h) above the blade. All velocities are shown in a blade-attached coordinate system, since that system is used for calculating blade loads. Additionally, the velocities were normalized by the blade-tip speed. As can be seen, the chordwise velocity component u is typically an order of magnitude larger than the vertical component v and the radial velocity w. Therefore, blade pressures and loads are a first-order function of u but depend on v and w only to second order. Thus, the good agreement between calculations and the experiments, especially for the strength and location of the shock waves, enhances confidence in the ROT22 code's ability to predict flowfields, pressures, and loads under the present conditions. Note, however, that the agreement with experiment is somewhat degraded at the blade tip. As a result of the steepness of the velocity gradients at the tip, the interpolation of the computed velocities in the radial direction reduced the resolution which diffused the shocks (see Figs. 6b and 6c).

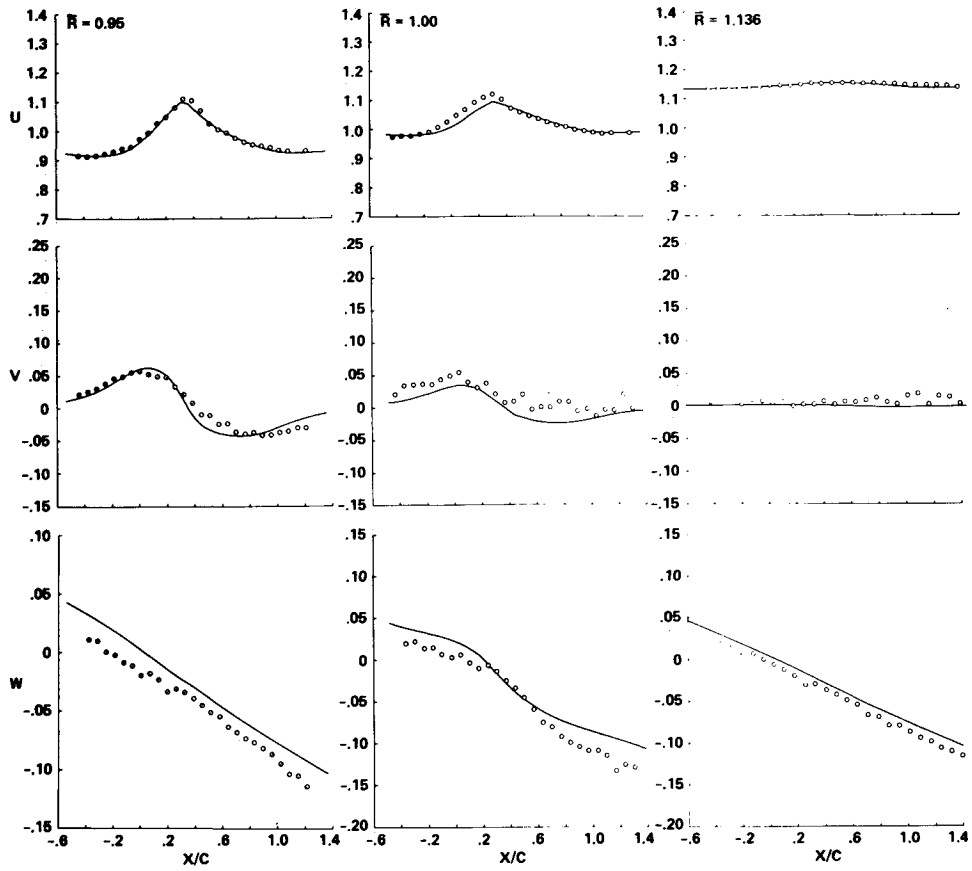

Fig. 6f Comparison of ROT22 calculated velocities with LV measurements: $M_{TIP} = 0.88$, $Y/C = 0.5172$.

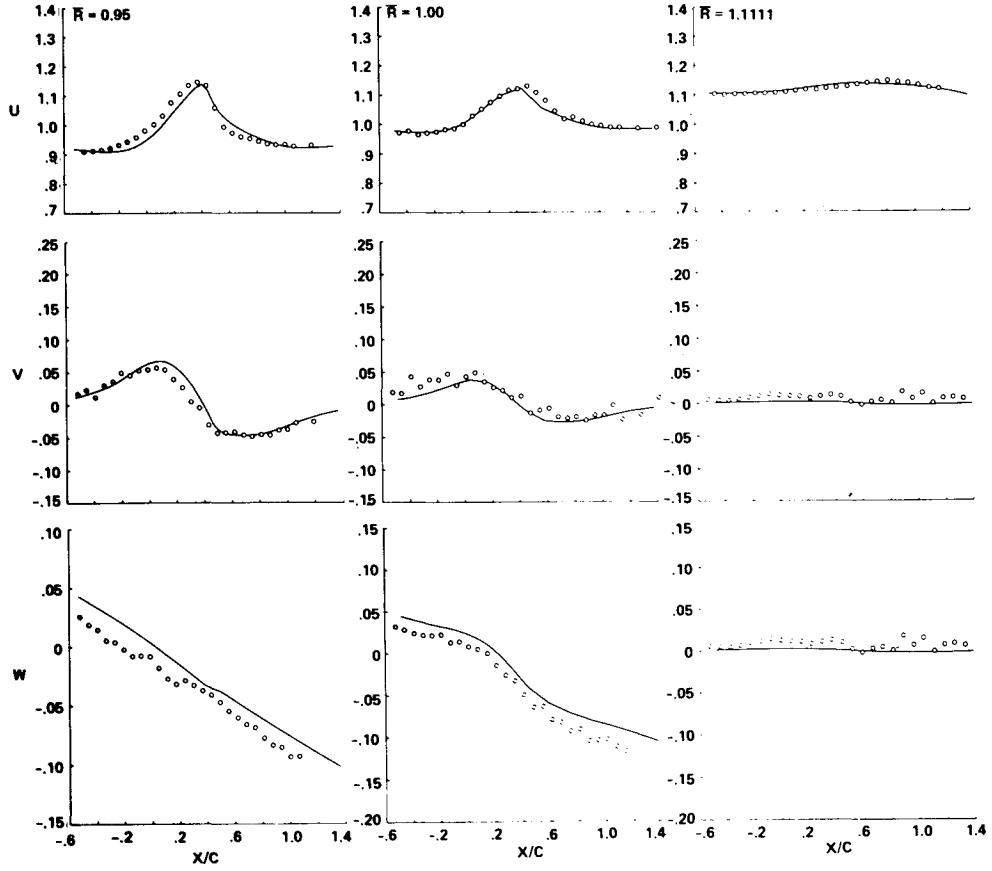

Fig. 6g Comparison of ROT22 calculated velocities with LV measurements: $M_{TIP} = 0.90$, $Y/C = 0.5172$.

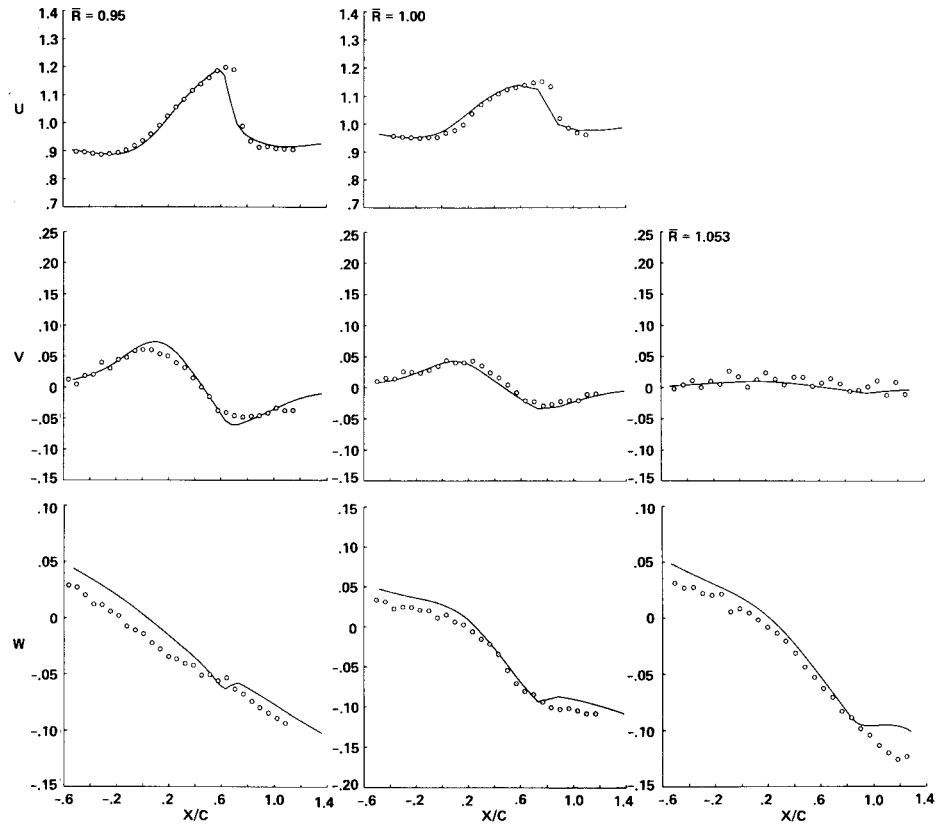

Fig. 6h Comparison of ROT22 calculated velocities with LV measurements: $M_{TIP}=0.95$, $Y/C=0.5172$.

The impulsive noise associated with the delocalization phenomemon is thought to be a result of the propagation of the shock forming on the blade into the far field.[5] Therefore, it was instructive to compare the LV data and the calculations at the sonic circle locations to see when the presence of shock waves was discernible. Note that the u velocity is the component most strongly affected by shock waves and that, as expected, the shocks were strongest close to the plane of the blade. At tip Mach numbers of 0.85 and 0.88, where delocalization was absent (Figs. 5a and 5b), no signs of shocks were visible (see Figs. 6b, 6e, and 6f). Even for a tip Mach number of 0.90, where delocalization occurred but was not extensive (Fig. 5c), no distinct shock was discernible at the sonic circle (see Figs. 6c and 6g). However, at the highest tip Mach number, 0.95, which caused extensive delocalization (Fig. 5d), the strong shock forming on the blade definitely propagated to the sonic circle region (Fig. 6d). In fact, the shock was still strong one-half chord above the plane of the blade (Fig. 6h), whereas no shock occurred at this location at tip Mach numbers below 0.90 (Figs. 6e and 6f). (The u-velocity component was not measured at the sonic circle at 0.95 tip Mach number. Therefore, the presence of the shock at the sonic circle in Fig. 6h can only be inferred from the radial velocity w distribution and the strength of the shock farther inboard.) The large increase in the shock strength that occurred at the tip Mach number of 0.95 lends support to the hypothesis of Ref. 5 that shock propagation into the far field occurs when strong delocalization is present.

Conclusions

It has been shown that a laser velocimeter can be used to measure accurately the velocities induced by a model rotor at transonic tip speeds. These extensive measurements yielded high-resolution orthogonal velocity components describing the flowfield. The velocities were used to illustrate the ability of the ROT22 code to predict accurately the transonic flowfield in the crucial region around and beyond the tip of a high-speed rotor blade. This supplements the comparisons of Ref. 4, where surface pressures were shown to be well predicted on two different tip geometries at advance ratios to 0.45.

Especially at the critical 90-deg azimuthal position, where delocalization was most likely to occur in forward flight, the angle of incidence in the tip region was small and had little effect on the flow beyond the tip. Therefore, the good agreement between calculated and LV-measured velocities, although for a nonlifting blade, indicates that the ROT22 code can be used with reasonable confidence to predict the important tip-region flowfield, including the occurrence, strength, and location of shock waves that cause high drag and noise.

References

[1]Arieli, R. and Tauber, M. E., "Computation of Subsonic and Transonic Flow about Lifting Rotor Blades," AIAA Paper 79-1667, 1979.

[2]Arieli, R. and Tauber, M. E., "Analysis of the Quasi-Steady Flow about an Isolated Lifting Helicopter Rotor Blade," Joint Institute for Aeronautics and Acoustics, Stanford University, Stanford, CA, TR-24, Aug. 1979.

[3]Owen, F. K., Orngard, G. M., and McDevitt, T. K., "Laser Velocimeter Measurements of Model Helicopter Rotor Flow Fields," NASA CR-177345, 1984.

[4]Tauber, M. E., Chang, I. C., Caughey, D. A., and Philippe, J. J., "Comparison of Calculated and Measured Pressures on Straight and Swept-Tip Model Rotor Blades," NASA TM-85872, 1983.

[5]Schmitz, F. H. and Yu, Y. H., "Transonic Rotor Noise: Theoretical and Experimental Comparison," Paper No. 22, 6th European Powered Lift Aircraft Forum, Bristol, England, Sept. 1980.

[6]Owen, F. K., "An Assessment of Flow-Field Simulation and Measurement," AIAA Paper 83-1721, 1983.

[7]Kittleson, J. K., "Holographic Interferometry Technique for Measuring Transonic Flow over a Rotor Blade," Paper No. B, 9th European Rotorcraft Forum, Stressa, Italy, Sept. 1983.

[8]Caradonna, F. X. and Isom, M. P., "Subsonic and Transonic Potential Flow over Helicopter Rotor Blades," *AIAA Journal*, Vol. 10, Dec. 1972, pp. 1606–1612.

[9]Caradonna, F. X. and Isom, M. P., "Numerical Calculation of Unsteady Transonic Potential Flow over Helicopter Rotor Blades," *AIAA Journal*, Vol. 14, April 1976, pp. 482–488.

[10]Grant, J., "Calculation of the Supercritical Flow over the Tip Region of a Non-Lifting Rotor Blade at Arbitrary Azimuth," Royal Aircraft Establishment, Farnborough, England, Tech. Rept. 77180, Dec. 1977.

[11]Jameson, A. and Caughey, D. A., "Numerical Calculation of the Transonic Flow past a Swept Wing," Courant Institute of Mathematical Sciences, New York University, New York, C00-3077-140, June 1977.

[12]Henne, P. A. and Hicks, R. M., "Wing Analysis Using a Transonic Potential Flow Computational Method," NASA TM-78464, July 1978.

[13]Egolf, T. A. and Sparks, P. S., "A Full Potential Rotor Analysis with Wake Influence Using an Inner-Outer Domain Technique," presented at the 42nd Annual Forum of the American Helicopter Society, Washington, DC, June 2–4, 1986.

[14]Tauber, M. E., "Computerized Aerodynamic Design of a Transonically Quiet Blade," Paper A-84-40-46, 40th Annual National Forum of the American Helicopter Society, Arlington, VA, May 1984.